



In-line gas chromatographic apparatus for measuring the hydrophobic micropore volume (HMV) and contaminant transformation in mineral micropores

Hefa Cheng^a, Martin Reinhard^{b,*}

^a State Key Laboratory of Organic Geochemistry, Guangzhou Institute of Geochemistry, Chinese Academy of Sciences, Guangzhou 510640, China

^b Department of Civil and Environmental Engineering, Stanford University, Stanford, CA 94305-4020, USA

ARTICLE INFO

Article history:

Received 21 November 2009

Received in revised form 26 February 2010

Accepted 10 March 2010

Available online 17 March 2010

Keywords:

Hydrophobic micropore volume (HMV)

Gas chromatographic apparatus

Sorption

Slow desorption

Transformation

Trichloroethylene

ABSTRACT

Desorption of hydrophobic organic compounds from micropores is characteristically slow compared to surface adsorption and partitioning. The slow-desorbing mass of a hydrophobic probe molecule can be used to calculate the hydrophobic micropore volume (HMV) of microporous solids. A gas chromatographic apparatus is described that allows characterization of the sorbed mass with respect to the desorption rate. The method is demonstrated using a dealuminated zeolite and an aquifer sand as the model and reference sorbents, respectively, and trichloroethylene (TCE) as the probe molecule. A glass column packed with the microporous sorbent is coupled directly to a gas chromatograph that is equipped with flame ionization and electron capture detectors. Sorption and desorption of TCE on the sorbent was measured by sampling the influent and effluent of the column using a combination of switching and injection valves. For geosorbents, the HMV is quantified based on Gurvitsch's rule from the mass of TCE desorbed at a rate that is characteristic for micropores. Instrumental requirements, design considerations, hardware details, detector calibration, performance, and data analysis are discussed along with applications. The method is novel and complements traditional vacuum gravimetric and piezometric techniques, which quantify the total pore volume under vacuum conditions. The HMV is more relevant than the total micropore volume for predicting the fate and transport of organic contaminants in the subsurface. Sorption in hydrophobic micropores strongly impacts the mobility of organic contaminants, and their chemical and biological transformations. The apparatus can serve as a tool for characterizing microporous solids and investigating contaminant–solid interactions.

© 2010 Elsevier B.V. All rights reserved.

1. Introduction

Hydrophobic micropores are pores with diameters less than 2.0 nm and with pore wall surface lacking of affinity for water [1,2]. Hydrophobic micropores of soils and aquifer materials (geosorbents) are of interest because they can be important sink for volatile organic compounds (VOCs) in the environment [1–9]. Desorption of VOCs from wet microporous solids typically occurs on two distinctly different time scales: (i) a short time scale during which the fast-desorbing fraction is removed from sites not associated with micropores, including vapor in inter-particulate void spaces and molecules adsorbed on external surfaces, or partitioned in the sorbed water film; and (ii) a long time scale caused by the slow-desorbing fraction that consists of molecules sequestered in micropores [3–6]. Mass transfer of the fast-desorbing fraction to surrounding aqueous phase is primarily controlled by retarded diffusion through water-filled mesopores (2–50 nm) [6]; in contrast,

the removal rate of the slow-desorbing fraction is controlled by hindered molecular diffusion in hydrophobic micropores [6,10].

Geosorbents consist predominantly of minerals with minor fractions contributed by organic matter. Micropores occur in both crystalline and amorphous minerals in the form of nano-scale pores, cavities, channels, and in micro-structures of mineral surfaces [11]. The scanning electron micrographs in Fig. 1 show the continuum of pore spaces from nanometer to sub-micron existing in minerals from aquifer sediment. Although often viewed as inert, the mineral matrix can significantly affect contaminant behavior, especially in geosorbents with low organic carbon content (<0.1%) [12]. A recent study observed a linear relationship between the microporosity of geosorbents and clay contents and concluded micropores are located mainly in the clay fraction [13].

The polarity of mineral surfaces is mainly determined by surface composition and charge distribution [14,15], a generalization that is presumably applicable to micropores. The large majority of mineral surfaces and therefore micropores exhibit strong affinity for water due to surface cations, under-coordinated oxygens, hydroxyl groups, and surface charge. In clay minerals, the surface polarity ranges from hydrophobic to hydrophilic; the uncharged

* Corresponding author. Tel.: +1 650 723 0308; fax: +1 650 723 7058.
E-mail address: reinhard@stanford.edu (M. Reinhard).

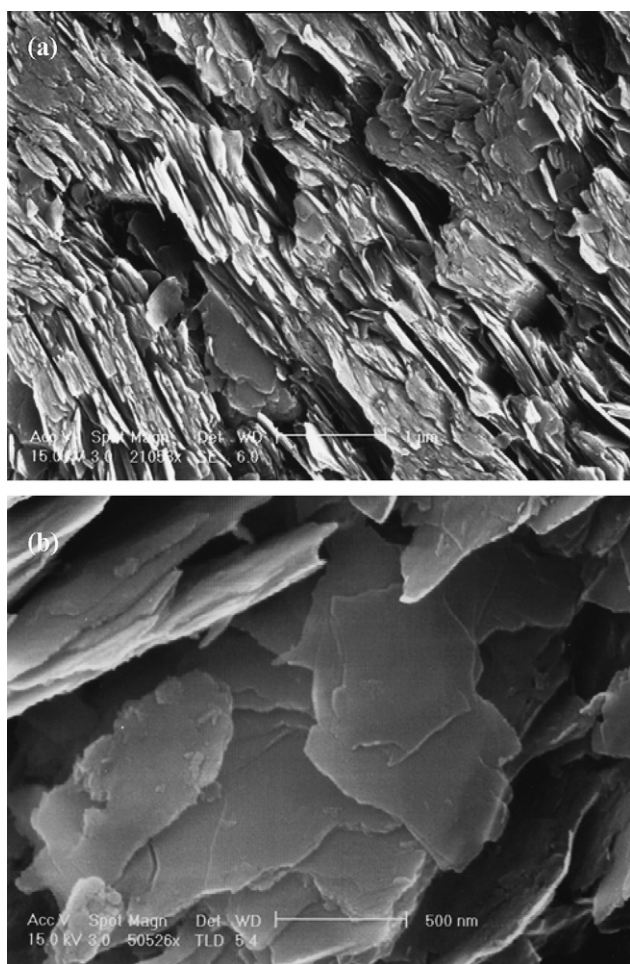


Fig. 1. Scanning electron micrographs showing the presence of pores ranging from nanometers to sub-microns in minerals from aquifer sediment: (a) aluminosilicate mineral particles not completely weathered to clay yet, and (b) clay platelets.

siloxane surfaces are hydrophobic, whereas the charged ones are hydrophilic [14,15]. Strong adsorption of water in hydrophilic pores prevents significant uptake of hydrophobic compounds [16,17]. Surfaces of hydrophobic pores are uncharged and lack hydrogen bonding sites, hence the free energy of water inside these pores is higher than in bulk water, which is in contrast to hydrophobic solutes, thus the latter can outcompete water for hydrophobic space inside the micropores [2,16,17]. Hydrophilic micropores are filled with water, even at low relative humidities (RHs), and hydrophobic solutes are excluded. Studies have shown that competition from water significantly reduces adsorption of hydrophobic organic contaminants in mineral micropores [2,5]. In spite of the polar nature of most mineral surfaces, a small fraction of the micropores present in geosorbents has been shown to be hydrophobic [1,2,18].

A generally accepted and standardized method for quantifying the hydrophobic micropore volumes (HMVs) of geosorbents and synthetic minerals does not appear to exist. Low temperature gas adsorption is used widely in characterizing the microporosity of solid materials [19]. Because gas adsorption is a vacuum-based technique that operates in the absence of water, the micropore volume that is accessible to hydrophobic compounds in the presence of water could not be quantified. Furthermore, the vacuum degassing pretreatment commonly used in gas adsorption could cause significant particle rearrangement and destruction of microporosity in geosorbents, particularly for clays [20,21]. The principle of determining HMV is based on (i) the ability of hydrophobic micropores to preferentially sorb hydrophobic compounds, such as trichloroethy-

lene (TCE), over water; and (ii) the slow-desorption kinetics of these compounds [1–7,17,22].

Here we detail instrumental requirements and design considerations of an in-line gas chromatographic apparatus that can be used for the quantification of the HMVs of microporous sorbents and propose using TCE as a probe molecule. Earlier communications have focused on applications of this apparatus [1,2,8,9]. This report specifies instrumental details, detector calibration, performance, and data analysis needed for the construction of such a system, and provides examples for its application.

2. Experimental

2.1. Instrumentation

The apparatus consisted of a gas supply system, a vapor generation component, a glass column packed with microporous sorbent housed in an oven, a combination of switching and injection valves for sampling, and a gas chromatograph (GC) for chemical analysis (Fig. 2). Although contaminant sorption–desorption kinetics can be calculated from batch uptake/release experiments [23], quantification of the micropore-sorbed fraction is difficult in batch systems [1,3–6]. Further, measuring low desorption flux from micropores in saturated aqueous systems is difficult as the solute concentration diminishes with time.

To overcome these limitations, a gas phase column apparatus was developed for measuring the sorption and desorption kinetics on microporous sorbents. After equilibration with water vapor at near 100% RH, the internal pores of solids up to 100 nm in size were filled by water [5]. Previous studies have shown that the total uptakes of organic sorbates by soils and sediments at above ~90% RH and under saturated conditions are similar [3–5]. Therefore, sorption and desorption of organic contaminants by microporous sorbents immersed in aqueous solutions can be studied by adjusting the gas phase RH to near 100%.

Helium was chosen as the purging gas because it is inert, and has a small atomic diameter (2.0 Å) and low polarizability (0.198 Å³). The flow rate was regulated by a digital mass flow controller with accuracy of ±1%. The gas stream was saturated with water vapor by bubbling helium through liquid water in a water saturator. Similarly, organic vapor was introduced into the helium stream by an organic saturator immersed in a refrigerated bath (±0.01 °C, Thermo Electron, Waltham, MA), with its concentration controlled by the bath's temperature. Condensation of the organic vapor in the system was avoided by operating the refrigerated bath at temperatures at least 4 °C below room temperature.

The sorption column (with a net volume of ~1.1 cm³) was made by joining two truncated glass pipettes by Teflon heat-shrink tube. It was housed inside an oven capable of heating at rates up to 70 °C/min. The column was coupled to an HP 5890-II gas chromatograph (Hewlett Packard, Palo Alto, CA) via an 8-port dead-end switching valve and a 10-port 2-position injection valve. The 8-port valve directed the column effluent to the GC detectors or to the 10-port valve, which injected the column influent and effluent alternatively into the GC column. The gas samples were analyzed by a flame ionization detector (FID) and an electron capture detector (ECD) connected in parallel. All gas flow lines were made of 0.53 mm o.d. fused silica capillary tubing (Supelco, Bellefonte, PA) and connected by fittings with fused silica adapters to prevent leakage. Glass and Teflon materials used minimized the interactions (e.g., chemical reaction and adsorption) with TCE. The GC and the 10-port valve were controlled by a computer running the GC ChemStation program (Agilent, Palo Alto, CA), which also acquired detector data at a frequency of 5.0 Hz. The digital mass flow controller and the 8-port valve were operated under manual control mode. Although

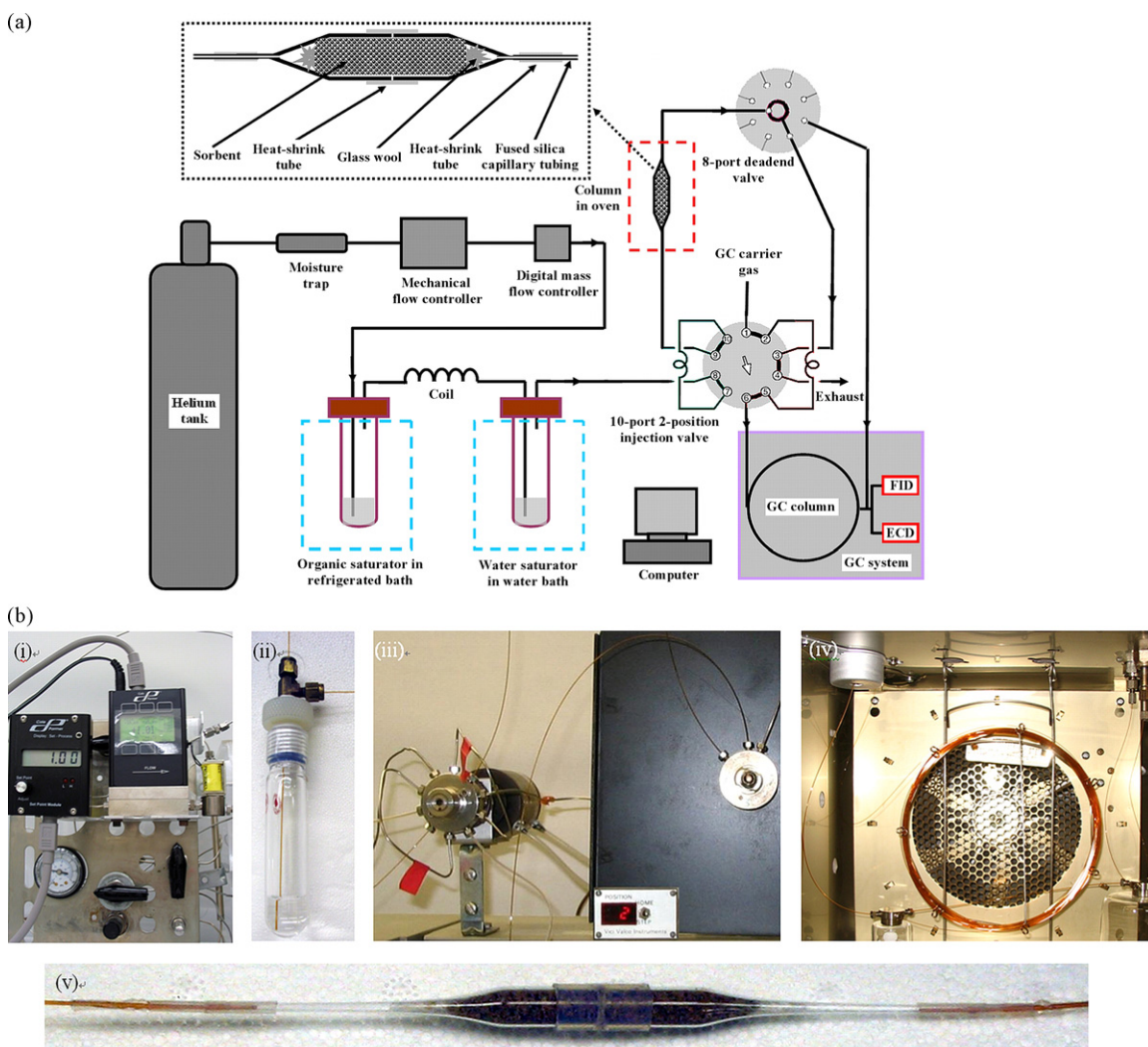


Fig. 2. Illustrations of the in-line gas chromatographic apparatus: (a) schematic flow diagram, and (b) key components of the apparatus. (i) digital mass flow controller (Cole-Parmer, Vernon Hills, IL), (ii) vapor saturator (adapted from 20 mL capillary column washer by Alltech, Deerfield, IL), (iii) 10-port 2-position injection valve with an air actuator (left) and 8-port dead-end switching valve with a standard electric actuator (right), both supplied by Valco (Houston, TX); (iv) DB-1 column (30 m × 0.32 mm × 0.25 μm, J & W Scientific, Folsom, CA) connected in parallel to FID and ECD; and (v) column packed with microporous sorbent. The sorption column was made by joining two truncated 5³/₄" borosilicate disposable pipettes (Fisher, Pittsburgh, PA) with 6.1 mm i.d. double-walled PTFE heat-shrink tube (Cole-Parmer, Vernon Hills, IL) after the sorbent was packed (without heating). The small ends of the pipettes were connected to the fused silica capillary tubing by 0.91 mm i.d. fluoroplastic PTFE/FEP dual shrink tube (Texloc, Fort Worth, Texas).

they could also be computer-controlled, the flow controller was always operated at 1.00 mL/min while the 8-port valve was only manually switched once during desorption.

In sorption and desorption experiments, the gas stream was sampled either by feeding the column effluent directly to the GC detectors or by injecting the column influent and effluent alternatively into the GC column. In continuous sampling, the detectors responded in real time to TCE flux. Continuous sampling was

optimal for measuring breakthrough curves and the flux of the fast-desorbing fraction. In discrete sampling, the TCE injected was chromatographically separated in the GC column and the mass detection was more accurate and sensitive. Discrete sampling produced data with a coarser time resolution (every 14 min for TCE), and was used to quantify the slow-desorbing flux. Multiple volatile organic species can be measured in the discrete sampling mode, making it possible to study of the transformation of organic com-

Table 1
Gas chromatographic conditions for studying TCE and 2,2-DCP sorption and desorption.

Sampling mode	Continuous sampling	Discrete sampling	
		TCE	2,2-DCP
Injection port temperature (°C)	130	130	130
Column head pressure (kPa)	160	160	160
Helium carrier flow rate (mL/min)	5.0	5.0	5.0
Column temperature (°C)	100 (isothermal)	100 (isothermal)	100 (isothermal)
FID temperature (°C)	300	300	300
ECD temperature (°C)	350	350	350
Compound retention time (min)	—	5.5 (TCE)	2.8 (2-CP) 3.6 (2,2-DCP)

pounds sorbed on microporous sorbents. General instrumental conditions used for performing the sorption and desorption experiments in this study are listed in Table 1.

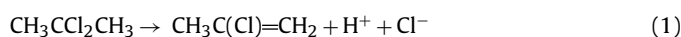
The experimental system used earlier [3–6] was improved by (i) providing better control of the organic vapor concentration in the gas stream through controlling the temperature of the organic saturator immersed in a refrigerated bath; and (ii) performing automated chemical analysis of the column influent and effluent using a computer-controlled sampling valve. The extremely low detection limits on halogenated hydrocarbons by ECD allowed acquisition of data in real time over the entire desorption profile without requiring sample concentration.

2.2. Sorbents

A highly microporous dealuminated Y zeolite, CBV-780 (Si/Al=40) was used as the model synthetic sorbent and a well-characterized sandy material from Borden aquifer (Ontario, Canada) was used as reference geosorbent. CBV-780, which is composed of 1–2 μm diameter crystals, was obtained from Zeolyst (Valley Forge, PA) and used as received. The micropore volume of CBV-780 is approximately 0.45 mL/g, close to its theoretical void volume fraction of 0.48 [2]. Micropores in the highly dealuminated CBV-780 are hydrophobic because dealumination decreases the framework surface charge, removes the surface cations, and converts surface silanol groups to nonpolar siloxane [24]. Borden aquifer material is a fine- to medium-grained sand composed largely of quartz and feldspars, with minor fractions of amphiboles and carbonates and a low organic carbon content of 0.021% [25]. Although the surface area of Borden sand is only 0.42 m^2/g , micropores contribute to a significant fraction of its sorption capacity and cause slow sorption kinetics [26]. A sample of Borden sand was dried by heating at 105 °C for 48 h. Samples of wet CBV-780 and Borden sand were prepared by equilibrating with water vapor at 100% RH above liquid water in a desiccator for at least 3 months at room temperature (24 ± 1 °C).

2.3. Sorbates

According to Gurvitsch's rule, the total micropore volume of a sorbent is independent of the sorbate provided that the amount adsorbed is expressed as the liquid volume and that selective effects are excluded [19]. Nonreactive compound TCE was chosen as the probing sorbate because it is of the appropriate size (average molecular diameter: 6.8 Å), has a relatively low polarity (0.77 Debye), and occurs widely in contaminated groundwater aquifers [27,28]. 2,2-Dichloropropane (2,2-DCP), which loses HCl and transforms into 2-chloropropene (2-CP) in the presence of water through a dehydrohalogenation reaction:



was selected as a reactive sorbate. The rate (3.18×10^{-4} 1/min at 24 °C) of this hydrolytic transformation reaction is pH-independent and is well suited for laboratory study [29].

2.4. System calibration and stability testing

The responses of the detectors were calibrated by injecting known amounts of TCE obtained by combinations of refrigerated bath temperature (–35, –20, and 0 °C) and sampling-loop size (5, 15, 20, 25, 50, and 100 μL) of the 10-port valve. Refrigerated bath temperature (–44 to 20 °C) and helium flow rate (0.25–10.0 mL/min) were varied to test the stability of TCE vapor concentration in the helium stream.

2.5. TCE and 2,2-DCP sorption and desorption

Glass columns were first packed with the model sorbents, with the masses determined by column weight differences. The column packed with dry Borden sand was conditioned in a 105 °C-oven (without flow), while those packed with wet solids were purged with a humidified (100% RH) helium stream for at least 2 h. During sorption, the dry column was fed with a stream of dry helium containing TCE vapor (505 $\mu\text{mol/L}$) at 1.00 mL/min (~ 1.4 pore volume/min); a humidified (100% RH) helium stream containing TCE vapor was used for the wet columns. The concentration of TCE in the column effluent was quantified by FID and/or ECD. The flow was stopped at full breakthrough and after being sealed the column was equilibrated in a 50 °C oven for 10 h. To study desorption, the column was purged with a dry or humidified (100% RH) helium stream at 1.00 mL/min while TCE concentration in the purge flow was measured. Temperature of the column oven was raised stepwise during later stage of desorption to accelerate the rate of desorption.

The transformation of 2,2-DCP in micropores of wet CBV-780 was also studied using the apparatus. First, 2,2-DCP was loaded onto wet CBV-780 by passing a humidified (100% RH) helium stream laden with 2,2-DCP vapor (1,106 $\mu\text{mol/L}$) through the column at 1.00 mL/min until full breakthrough. The column was then sealed off and heated at 50 °C for 382.2 h. After heat treatment the column was cooled immediately to room temperature, re-connected, and purged with a humidified (100% RH) helium stream at 1.00 mL/min. Concentrations of 2,2-DCP and its transformation product, 2-CP, in the column effluent were analyzed using the discrete sampling mode during desorption, and stepwise temperature increases were made to accelerate the desorption rates in the later stage.

2.6. Data analysis

The total mass of TCE retained in the column (M_{tot}) was comprised of four fractions: adsorbed on external surfaces (M_{surf}), vapor in the large inter-particulate void spaces (M_{vapor}), partitioned in the sorbed water film (M_{part} , this fraction did not exist in the absence of water), and sorbed in the micropores (M_{micro}):

$$M_{\text{tot}} = M_{\text{surf}} + M_{\text{vapor}} + M_{\text{part}} + M_{\text{micro}} \quad (2)$$

M_{tot} was calculated by integrating the area above the acquired breakthrough curve after subtracting the area attributed to the system dead volume:

$$M_{\text{tot}} = \int_{t_1}^{t_2} Q [C_0 - C(t)] dt \quad (3)$$

where t_1 is the breakthrough time without column, t_2 is the breakthrough time for the packed column, C_0 and $C(t)$ represent the influent and measured effluent TCE concentrations, and Q is the helium flow rate. The system dead volume, which is the sum of volumes extraneous to the column in the flow path, was obtained by blank runs without column (the slopes of the breakthrough curves were vertical).

For a sorbent with high microporosity, M_{micro} was much larger than the sum of M_{surf} , M_{vapor} , and M_{part} . Consequently, $M_{\text{tot}} \approx M_{\text{micro}}$ since practically all TCE retained in the column could be attributed to sorption in micropores. In contrast, for low microporosity geosorbents, only a small fraction of the total retained TCE was sorbed in the micropores ($M_{\text{micro}} \ll M_{\text{tot}}$), and micropore-sorbed mass could only be quantified from the slow-desorbing flux. This required fitting the desorption data to a kinetic micropore desorption model to obtain the mass remaining (in micropores) at the transition from fast- to slow-desorption. A radial diffusion model, either alone or coupled with the advection-dispersion equation [7], was used. Details on model derivation, equations, boundary and ini-

tial conditions can be found in Li and Werth [7] and are not repeated here (note: the correct expression for equation 7f in Li and Werth [7] should be: $q(x, \bar{r}, t) = C(x, t)/K_v$). The numerical method was set up and tested following procedures similar to those described previously [1,7], and best model fits were obtained by minimizing the sum of the relative least-squared errors between the model results and the experimental data.

The radial diffusion model coupled with the advection-dispersion equation was used to model the first desorption stage. For the second desorption stage, the mass transfer limitations external to solid particles were insignificant and the radial diffusion model with a γ distribution of diffusion rate constants was sufficient to describe the slow desorption from micropores [1,7]. The point where the two modeled curves meet represents the transition from fast- to slow-desorption (t_3). Consequently, the mass desorbed from this point to the end of desorption measurement (t_4) was taken as the mass resided in the micropores:

$$M_{\text{micro}} = \int_{t_3}^{t_4} QC(t)dt \quad (4)$$

The HMV was calculated from the micropore-sorbed TCE mass (M_{micro} , obtained from either the breakthrough curve or the slow-desorbing flux) based on Gurvitsch's rule [19] with the assumption that its density in the micropores was the same as that in bulk liquid (ρ_{liq}):

$$V_{\text{micro}} = \frac{M_{\text{micro}}}{\rho_{\text{liq}}} \quad (5)$$

For geosorbents, the fast-desorbing fraction was typically purged from the column in relatively short times (<1 h), while desorption of the micropore-sorbed fraction lasted days. TCE masses in the fast- and slow-desorbing fractions corresponded to those removed in the first and second desorption stages, respectively. V_{micro} obtained under dry conditions was deemed as the total micropore volume of the geosorbent, while that under wet conditions as the volume of hydrophobic micropores (i.e., HMV).

3. Results and discussion

3.1. System calibration and stability of vapor generation

Fig. 3 shows the responses of FID and ECD to TCE concentration during system calibration. FID responded linearly over three orders of TCE concentrations. In the continuous sampling mode, the response of FID was also found to be a linear function of TCE flux (data not shown). Compared to FID, ECD provided more than one order of magnitude higher sensitivity for TCE. However, its response was non-linear and the calibration curve was fitted to a power function.

It is critical that during sorption experiments the TCE concentration in the column feed is accurately known and constant. Fig. 4a shows the influence of the refrigerated bath temperature on TCE vapor concentration in the gas stream. The measurement results between -40 and 20 °C agree well with the quasi-polynomial equation predictions from the Korean Thermophysical Properties Data Bank [30]. The vapor pressure of TCE varied by almost two orders over the temperature range of -40 – 20 °C, thus helium stream with a wide range of TCE concentrations could be obtained by controlling the refrigerated bath temperature.

Fig. 4b shows the influence of helium flow rate on TCE vapor concentration at -40 , 4 , and 10 °C. TCE concentration remained constant as the flow rate increased from 0.25 to 10.0 mL/min at all three temperatures. These results demonstrate that mass transfer from liquid to gas phase was not a limiting factor for TCE evaporation under the system's operating conditions, and that the TCE

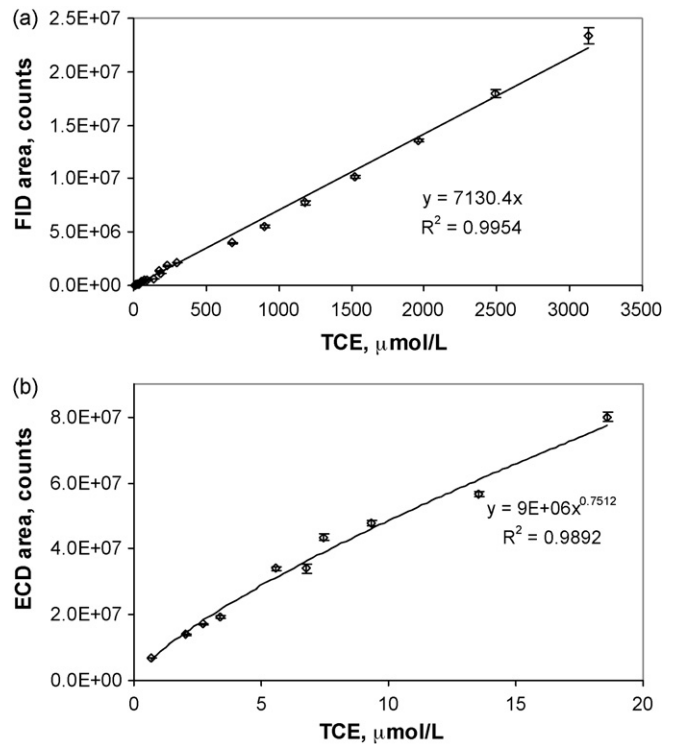


Fig. 3. Calibration curves for (a) FID, and (b) ECD. Error bars represent 99.7% confidence intervals ($n=20$).

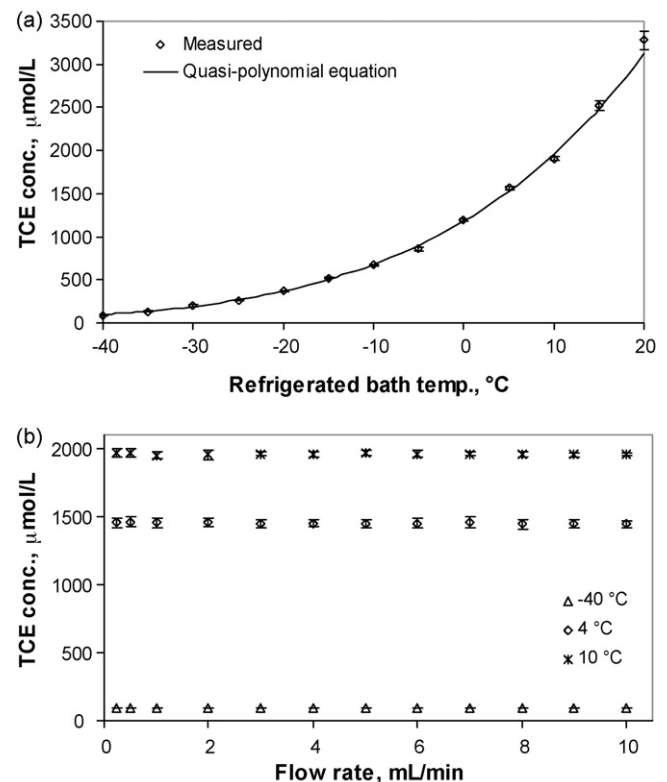


Fig. 4. Influence of (a) refrigerated bath temperature, and (b) purging gas flow rate on TCE vapor concentration. Error bars represent 99.7% confidence intervals ($n=20$).

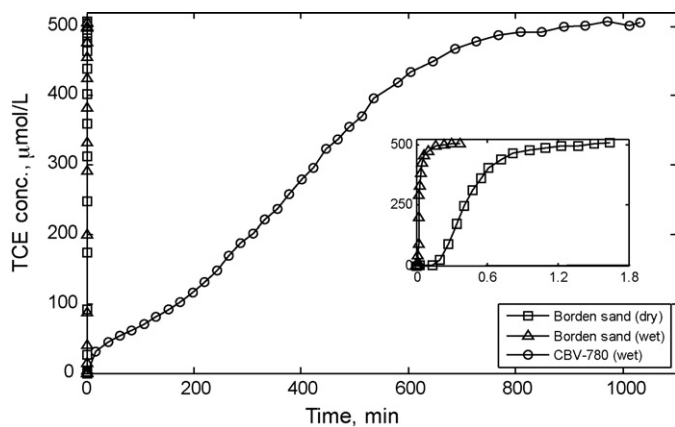


Fig. 5. Breakthrough curves of TCE vapor on wet CBV-780 and Borden sand, and dry Borden sand (normalized to 0.2 g dry solid) at 24 °C, with the inset showing a magnified view for dry and wet Borden sand. Dry (for dry Borden sand) or humidified (100% RH, for wet CBV-780 and Borden sand) helium with TCE vapor ($C_0 = 505 \mu\text{mol/L}$, or $P/P_0 = 0.136$) was passed through the column at 1.00 mL/min during sorption. Data were acquired every 0.2 s during continuous sampling and every 14 min during discrete sampling. Only selected data points are shown in the figure.

vapor in the helium stream was always in equilibrium with the bulk liquid.

3.2. Quantifying the HMV from breakthrough curve for highly microporous sorbent

Fig. 5 shows the TCE vapor sorption breakthrough curves on wet CBV-780 and Borden sand, and dry Borden sand. Breakthrough of TCE on dry and wet Borden sand occurred almost instantaneously, while full TCE breakthrough on wet CBV-780 took approximately 1000 min. TCE uptakes calculated from these breakthrough curves (after subtracting the negligible system dead space volume) were 932, 1.20, and 0.19 $\mu\text{mol/g}$ for wet CBV-780, dry Borden sand, and wet Borden sand, respectively. On the highly microporous CBV-780, the amounts of organic compounds resided outside of micropores were negligible compared to those sorbed within the micropores [2,8]. Hence, all TCE retained could be assumed to be sorbed in the micropores (i.e., $M_{\text{tot}} \approx M_{\text{micro}}$). The micropores in wet CBV-780 had been completely filled by water prior to TCE adsorption, thus the significant TCE uptake could only be explained by the displacement of water from the hydrophobic micropore spaces by TCE [2]. Based on the mass of TCE sorbed, the HMV of CBV-780 was estimated to be 83.8 $\mu\text{L/g}$, or 18.6% of the total micropore volume. This is in agreement with the fact that dealuminated zeolites with high silica contents ($\text{Si/Al} > 8$) are hydrophobic [10].

On the dry and wet Borden sands, the TCE uptakes by their micropores were relatively small, and the compartments (external surfaces, inter-particulate void spaces, and sorbed water film) other than micropores contributed significantly to the total mass retained. In these cases, the mass of TCE that resided outside of micropores was significant ($M_{\text{surf}} + M_{\text{vapor}} + M_{\text{part}} \gg M_{\text{micro}}$), making it necessary to differentiate the micropore-sorbed TCE from the total by measuring the desorption profile and quantifying the slow-desorbing flux.

3.3. Quantifying the HMV from desorption profile for low microporosity sorbent

Fig. 6a shows the desorption profiles of TCE on dry and wet Borden sand. Two-stage desorption behavior was observed in both cases, with desorbed TCE concentration decreasing rapidly at the beginning of desorption and then gradually leveling off. Near complete desorption of TCE from dry and wet Borden sand took

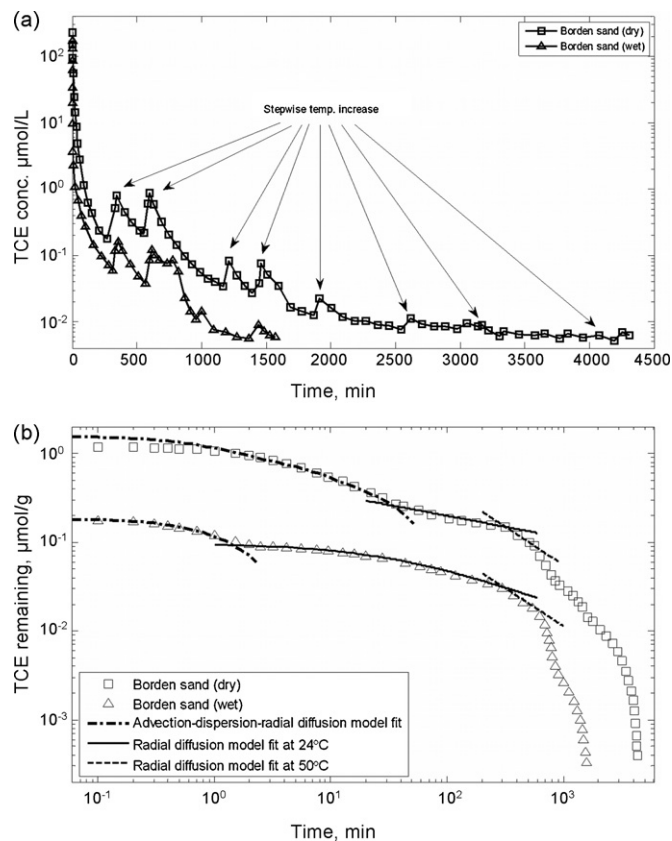


Fig. 6. TCE desorption from dry and wet Borden sand: (a) TCE concentration in the purge flow plotted as a function of time, and (b) TCE mass remaining, along with the model-fitted desorption profiles at 24 and 50 °C. Pulses in desorption flux (indicated by the arrows for dry Borden sand) shown in (a) was caused by stepwise increases in desorption temperature (first to 50 °C and then with 25 °C increment in each step followed). Data were acquired every 0.2 s during continuous sampling and every 14 min during discrete sampling. Only selected data points are shown in the figures.

approximately 4400 and 1600 min, respectively. Borden sand does not possess intraparticle micropores except for possible cracks and pits on the grain surfaces caused by weathering. Within these micropores, the spaces surrounded by uncharged siloxane surfaces are hydrophobic [1,22]. The fast-desorbing fraction consisting of TCE adsorbed on the external surfaces and resided in large interparticulate void space as vapor (and also partitioned in the adsorbed water film on the wet Borden sand), was purged from the column relatively quickly. The slow-desorbing fraction resulted exclusively from the mass desorbing from micropores where molecular diffusion was limited by steric hindrance and elevated activation energy for desorption [6,19]. Comparison of TCE sorption on dry and wet Borden sand indicates much weaker sorption under wet conditions, which is attributed to strong competition from water molecules for hydrophilic surfaces and micropore spaces. Stepwise increases in the column temperature caused pulses in the desorption flux, as expected, because of higher micropore diffusion rates at higher temperatures [1,6].

The two-stage desorption behavior characteristic of microporous solids [4–7] are evident in the mass remaining profiles (Fig. 6b). The two-stage desorption behavior observed here suggests that most of the TCE mass was sorbed extraneous to micropores. The first and second desorption stages could be fitted with a radial diffusion model in conjunction with the advection-dispersion equation or a radial diffusion model alone, respectively [1,7]. Removal of the fast-desorbing TCE from dry and wet Borden sand occurred in approximately 35.0 and 1.8 min, respectively, and the masses desorbed from micropores was believed to be negligible

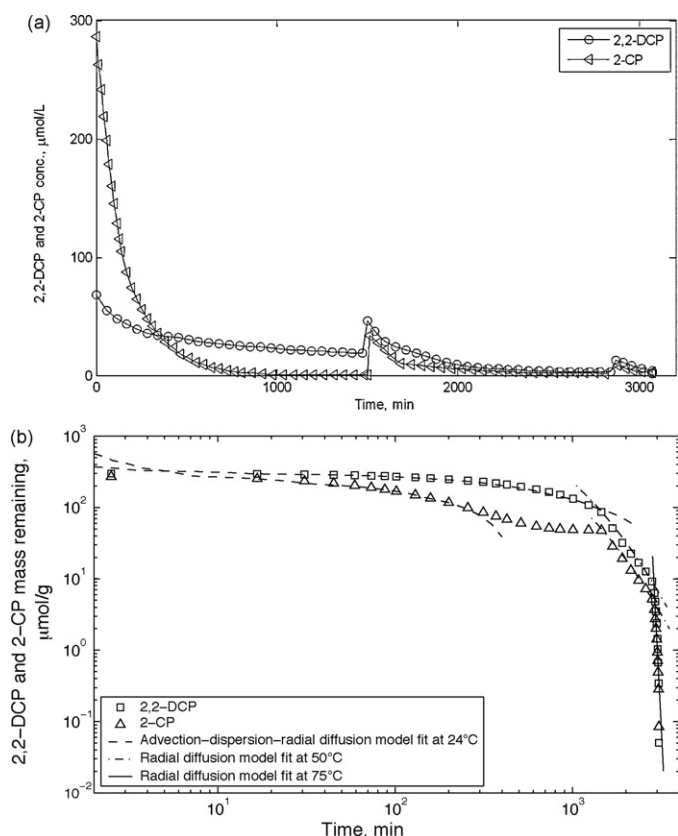


Fig. 7. 2,2-DCP and 2-CP desorption from wet CBV-780 after 382.2-h incubation at 50 °C: (a) 2,2-DCP and 2-CP concentrations in the purge flow plotted as a function of time, and (b) mass remaining profiles along with the model fits. Data were acquired every 0.2 s during continuous sampling and every 14 min during discrete sampling. Only selected data points are shown in the figures.

during these short periods, in relation to both the fast-desorbing and the micropore-sorbed fractions. The mass contained in the slow-desorbing fraction of dry Borden sand and the hydrophobic micropores on wet Borden sand were 0.278 and 0.097 μmol/g, respectively. Based on the molecular volume of TCE (90 mL/mol), the total and hydrophobic micropore volumes of Borden sand were estimated to be 2.6×10^{-2} and 8.7×10^{-3} μL/g, respectively. Compared to CBV-780, Borden sand exhibited very low micropore sorption capacities for TCE under both dry and wet conditions, as expected from its low microporosity. A relatively high proportion (34.9%) of the total micropore volume is hydrophobic, probably because a significant fraction of the micropores is located within quartz grains surrounded by the relatively hydrophobic siloxane surfaces.

3.4. Quantifying transformation of reactive compound in micropores

Fig. 7a shows the desorption profiles of 2,2-DCP and its dehydrohalogenation product, 2-CP, from wet CBV-780. Desorption of organic molecules from the hydrophobic CBV-780 was significantly different from that from the hydrophilic sorbents in that no rapid concentration decrease was observed. With a hydrolysis half-life of 1.06 h at 50 °C, complete transformation of 2,2-DCP to 2-CP would have occurred in aqueous solution after 382.2 h [29], while the desorption results clearly show that most of the 2,2-DCP remained untransformed in the micropores of CBV-780.

Experimental and model-fitted mass remaining profiles of 2,2-DCP and 2-CP on wet CBV-780 are presented in Fig. 7b. The absence of two-stage desorption behavior resulted from the high micropore

diffusion rates in the zeolite with a large HMV, and such behavior has also been previously reported for a high silica (Si/Al = 65) zeolite H-ZSM-5 [7]. A radial diffusion model coupled with the advection-dispersion equation adequately described 2,2-DCP desorption [7,8]. 2-CP desorption profile from CBV-780 was significantly different from that of 2,2-DCP, presumably because its formation was heterogeneous in the micropore spaces limited by the availability of reactive water [8]. Enhancements in 2,2-DCP and 2-CP desorption fluxes were also observed with step increases in column desorption temperature.

Because of the much faster 2,2-DCP transformation rate expected at 50 °C than at room temperature [29], 2,2-DCP transformation during the sorption and desorption processes was considered insignificant [8,9]. The total masses of 2,2-DCP and 2-CP desorbed were 298.9 and 273.2 μmol/g, respectively, which account for 97.8% of the sorbed mass (585.2 μmol/g, determined from sorption breakthrough measurement). In the water-filled micropores of CBV-780, only 47.7% 2,2-DCP transformed to 2-CP after reaction at 50 °C for 382.2 h whereas complete 2,2-DCP transformation would have occurred in bulk water. These results indicate that hydrolytic transformation of 2,2-DCP in hydrophobic micropores was significantly inhibited due to the limited availability of reactive water, which has important implications on the fate of reactive contaminants in the subsurface environment [8,9].

4. Conclusion

A gas chromatographic apparatus was developed for determining the mass sorbed in hydrophobic micropores through measuring the sorption breakthrough curve and desorption profile of a volatile organic compound (TCE) under controlled humidity and temperature. By analyzing the breakthrough curve and the desorption profile, the HMV can be quantified from the TCE mass sorbed in the micropores in the presence of water vapor at 100% RH. Measurement results for a dealuminated Y zeolite and an aquifer sand agree with their structural and compositional properties and literature information. Automated in-line analysis provides the capability to obtain reliable results from unattended experiments without manual sampling. This system can characterize the micropore sorption capacity of geosorbents under environmentally relevant conditions instead of high vacuum. TCE has been used as a probe molecule because it is stable, can easily be detected using gas chromatographic detectors, and is of the appropriate size. The HMV of geosorbent is more relevant than the total micropore volume for predicting the fate and transport of VOCs in subsurface. The apparatus functioned well over a period of four years and produced some exciting research data [1,2,8,9], demonstrating its robustness and capability as a versatile tool for characterizing the HMVs of geosorbents and for studying the transformation of organic contaminants in the micropores.

Acknowledgement

This study was funded by the U.S. Environmental Protection Agency under project R828772-01 through the Western Region Hazardous Substance Research Center (Oregon State University, Corvallis, OR, and Stanford University, Stanford, CA). H. C. gratefully acknowledges the financial support from the "One Hundred Talents" program of the Chinese Academy of Sciences. We thank the anonymous reviewers for helpful comments. This is contribution No. IS-1174 from GIGCAS.

References

- [1] H. Cheng, M. Reinhard, Measuring hydrophobic micropore volumes in geosorbents from trichloroethylene desorption data, *Environ. Sci. Technol.* 40 (11) (2006) 3595–3602.

- [2] H. Cheng, M. Reinhard, Sorption of trichloroethylene in hydrophobic micropores of dealuminated Y zeolites and natural minerals, *Environ. Sci. Technol.* 40 (24) (2006) 7694–7701.
- [3] J. Farrell, M. Reinhard, Desorption of halogenated organics from model solids, sediments, and soil under unsaturated conditions. 1. Isotherms, *Environ. Sci. Technol.* 28 (1) (1994) 53–62.
- [4] J. Farrell, M. Reinhard, Desorption of halogenated organics from model solids, sediments, and soil under unsaturated conditions. 2. Kinetics, *Environ. Sci. Technol.* 28 (1) (1994) 63–72.
- [5] P. Grathwohl, M. Reinhard, Desorption of trichloroethylene in aquifer material: rate limitation at the grain scale, *Environ. Sci. Technol.* 27 (12) (1993) 2360–2366.
- [6] C.J. Werth, M. Reinhard, Effects of temperature on trichloroethylene desorption from silica gel and natural sediments. 2. Kinetics, *Environ. Sci. Technol.* 31 (3) (1997) 697–703.
- [7] J. Li, C.J. Werth, Slow desorption mechanisms of volatile organic chemical mixtures in soil and sediment micropores, *Environ. Sci. Technol.* 38 (2) (2004) 440–448.
- [8] H. Cheng, M. Reinhard, Sorption and inhibited dehydrohalogenation of 2,2-dichloropropane in micropores of dealuminated Y zeolites, *Environ. Sci. Technol.* 41 (6) (2007) 1934–1941.
- [9] H. Cheng, M. Reinhard, The rate of 2,2-dichloropropane transformation in mineral micropores: Implications of sorptive preservation for fate and transport of organic contaminants in the subsurface, *Environ. Sci. Technol.* 42 (8) (2008) 2879–2885.
- [10] D.M. Ruthven, *Principles of Adsorption and Adsorption Processes*, John Wiley, New York, 1984, p. 464.
- [11] J.B. Dixon, D.G. Schulze (Eds.), *Soil Mineralogy with Environmental Applications*, Soil Science Society of America, Inc., Madison, Wisconsin, 2002, p. 866.
- [12] G.P. Curtis, P.V. Roberts, M. Reinhard, A natural gradient experiment on solute transport in a sand aquifer. 4. Sorption of organic solutes and its influence on mobility, *Water Resour. Res.* 22 (13) (1986) 2059–2067.
- [13] R. Aringhieri, Nanoporosity characteristics of some natural clay minerals and soils, *Clays Clay Miner.* 52 (6) (2004) 700–704.
- [14] W.F. Jaynes, S.A. Boyd, Hydrophobicity of siloxane surfaces in smectites as revealed by aromatic hydrocarbon adsorption from water, *Clays Clay Miner.* 39 (4) (1991) 428–436.
- [15] G. Sposito, N.T. Skipper, R. Sutton, S.H. Park, A.K. Soper, J.A. Greathouse, Surface geochemistry of the clay minerals, *Proc. Natl. Acad. Sci. USA* 96 (7) (1999) 3358–3364.
- [16] E.A. Muller, F.R. Hung, K.E. Gubbins, Adsorption of water vapor-methane mixtures on activated carbons, *Langmuir* 16 (12) (2000) 5418–5424.
- [17] J. Luo, J. Farrell, Examination of hydrophobic contaminant adsorption in mineral micropores with grand canonical Monte Carlo simulations, *Environ. Sci. Technol.* 37 (9) (2003) 1775–1782.
- [18] L.S. Hundal, M.L. Thompson, D.A. Laird, A.M. Carmo, Sorption of phenanthrene by reference smectites, *Environ. Sci. Technol.* 35 (17) (2001) 3456–3461.
- [19] S.J. Gregg, K.S.W. Sing, *Adsorption, Surface Area and Porosity*, Academic Press, London, 1982, p. 303.
- [20] R.S. Murray, J.P. Quirk, Surface area of clays, *Langmuir* 6 (1) (1990) 122–124.
- [21] A. Neaman, M. Pelletier, F. Villieras, The effects of exchanged cation, compression, heating and hydration on textural properties of bulk bentonite and its corresponding purified montmorillonite, *Appl. Clay Sci.* 22 (4) (2003) 153–168.
- [22] J. Farrell, B. Hauck, M. Jones, Thermodynamic investigation of trichloroethylene adsorption in water-saturated microporous adsorbents, *Environ. Toxicol. Chem.* 18 (8) (1999) 1637–1642.
- [23] J.A. Cunningham, J.J. Deitsch, J.A. Smith, M. Reinhard, Quantification of contaminant sorption-desorption time-scales from batch experiments, *Environ. Toxicol. Chem.* 24 (9) (2005) 2160–2166.
- [24] N.Y. Chen, Hydrophobic properties of zeolites, *J. Phys. Chem.* 80 (1) (1976) 60–64.
- [25] W.P. Ball, P.V. Roberts, Long-term sorption of halogenated organic chemicals by aquifer material. 1. Equilibrium, *Environ. Sci. Technol.* 25 (7) (1991) 1223–1237.
- [26] W.P. Ball, P.V. Roberts, Long-term sorption of halogenated organic chemicals by aquifer material. 2. Intraparticle diffusion, *Environ. Sci. Technol.* 25 (7) (1991) 1237–1249.
- [27] H. Cheng, D.A. Sabatini, T.C.G. Kibbey, Solvent extraction for separating micellar-solubilized contaminants and anionic surfactants, *Environ. Sci. Technol.* 35 (14) (2001) 2995–3001.
- [28] M.G. Davie, H. Cheng, G.D. Hopkins, C.A. LeBron, M. Reinhard, Implementing heterogeneous catalytic dechlorination technology for remediating TCE-contaminated groundwater, *Environ. Sci. Technol.* 42 (23) (2008) 8908–8915.
- [29] P.M. Jeffers, L.M. Ward, L.M. Woytowitch, N.L. Wolfe, Homogeneous hydrolysis rate constants for selected chlorinated methanes, ethanes, ethenes, and propanes, *Environ. Sci. Technol.* 23 (8) (1989) 965–969.
- [30] Chemical Engineering Research Information Center. The Korea Thermophysical Properties Data Bank (KDB), April 3, 2007.